Immunity
Article

Continuous Expression of the Transcription Factor E2-2 Maintains the Cell Fate of Mature Plasmacytoid Dendritic Cells

Hiyaa S. Ghosh,[1,2] Babacar Cisse,[1,2,3] Anna Bunin,[1] Kanako L. Lewis,[1] and Boris Reizis[1,*]
[1]Department of Microbiology and Immunology, Columbia University Medical Center, New York, NY 10032, USA
[2]These authors contributed equally to this work
[3]Present address: Department of Neurological Surgery, Weill Cornell Medical College, New York, NY 10065, USA
*Correspondence: bvr2101@columbia.edu
DOI 10.1016/j.immuni.2010.11.023

SUMMARY

The interferon-producing plasmacytoid dendritic cells (pDCs) share common progenitors with antigen-presenting classical dendritic cells (cDCs), yet they possess distinct morphology and molecular features resembling those of lymphocytes. It is unclear whether the unique cell fate of pDCs is actively maintained in the steady state. We report that the deletion of transcription factor E2-2 from mature peripheral pDCs caused their spontaneous differentiation into cells with cDC properties. This included the loss of pDC markers, increase in MHC class II expression and T cell priming capacity, acquisition of dendritic morphology, and induction of cDC signature genes. Genome-wide chromatin immunoprecipitation revealed direct binding of E2-2 to key pDC-specific and lymphoid genes, as well as to certain genes enriched in cDCs. Thus, E2-2 actively maintains the cell fate of mature pDCs and opposes the "default" cDC fate, in part through direct regulation of lineage-specific gene expression programs.

INTRODUCTION

Dendritic cells (DCs) of the immune system efficiently recognize pathogens through pattern recognition receptors such as Toll-like receptors (TLRs), secrete multiple cytokines, and activate naive T cells during primary responses. The latter property distinguishes them among other innate immune cell types and establishes a key link between innate and adaptive immunity (Steinman and Idoyaga, 2010). In humans and in experimental animals, DCs are represented by two major lineages, classical or conventional DCs (cDCs) and plasmacytoid DCs (pDCs) (Merad and Manz, 2009). The cDCs show high surface expression of MHC class II (MHC II) and of the integrin CD11c, and even in the steady state have outstanding capacity for naive T cell priming. Murine cDCs comprise two phenotypically and functionally distinct subsets, distinguished by surface expression of CD8α in the lymphoid organs and CD103 in tissues; similar subsets have been proposed for the human cDCs (Shortman and Heath, 2010). In contrast, pDCs are specialized in TLR-mediated recognition of viral nucleic acids and high-level secretion of type I interferon (IFN) in response to viruses (Liu, 2005; Swiecki and Colonna, 2010). The unique IFN secretion capacity of pDCs is facilitated by baseline expression of IRF7, the transcriptional "master regulator" of IFN response; conversely, it is tightly controlled by pDC-specific inhibitory receptors such as human ILT7 and BDCA-2 and murine Siglec-H (Gilliet et al., 2008). The pDCs express low MHC II and CD11c and display distinct markers such as CD45RA (also known as B220), Ly-6c, and Bst2, which is highly specific for murine pDCs in the steady state (Blasius et al., 2006) and also serves as ILT7 ligand in humans (Cao et al., 2009). The pDCs in the steady state have poor T cell stimulatory capacity, whereas upon activation by viruses and TLR ligands, they can efficiently present and cross-present Ag to T cells (Villadangos and Young, 2008).

Multiple lines of evidence suggest that cDCs and pDCs are closely related. First, both lineages are postulated to develop in the same pathway (Liu and Nussenzweig, 2010) from a bone marrow (BM) progenitor termed common DC progenitor (CDP) or pro-DC (Naik et al., 2007; Onai et al., 2007). This common developmental pathway critically depends on cytokine Flt3 ligand (Flt3L), its receptor Flt3, and downstream transcription factor Stat3 (Schmid et al., 2010). Second, genome-wide expression profiles of human and murine pDCs are most similar to those of the respective cDCs but distinct from lymphocytes or myeloid cells (Robbins et al., 2008). Third, in vitro activation by viruses or cytokines induces human pDC differentiation into cells with morphological and functional properties of cDCs (Soumelis and Liu, 2006). In contrast, pDCs differ from cDCs in several key aspects. Most obviously, cDCs exhibit typical DC morphology with prominent cytoplasmic veils and protrusions (dendrites), whereas pDCs have round morphology of a secretory lymphocyte. Indeed, pDCs display many salient features of lymphocytes such as relatively long lifespan on the order of weeks, contrasted with cDC turnover within several days (Liu et al., 2007; O'Keeffe et al., 2002). In particular, pDCs show important molecular similarities with B lymphocytes, including shared markers (B220), nucleic acid-sensing TLRs (TLR7, TLR9), transcription factors (SpiB, Bcl11a), and a B cell receptor (BCR)-like signaling pathway that inhibits IFN secretion (Crozat et al., 2010; Gilliet et al., 2008). Moreover, pDCs express B cell-specific pIII isoform of MHC II transactivator CIITA, in contrast to the pI isoform expressed exclusively by cDCs (LeibundGut-Landmann et al., 2004). Finally, pDCs express multiple transcripts specific for developing T and B lymphocytes, such as human *PTCRA* and

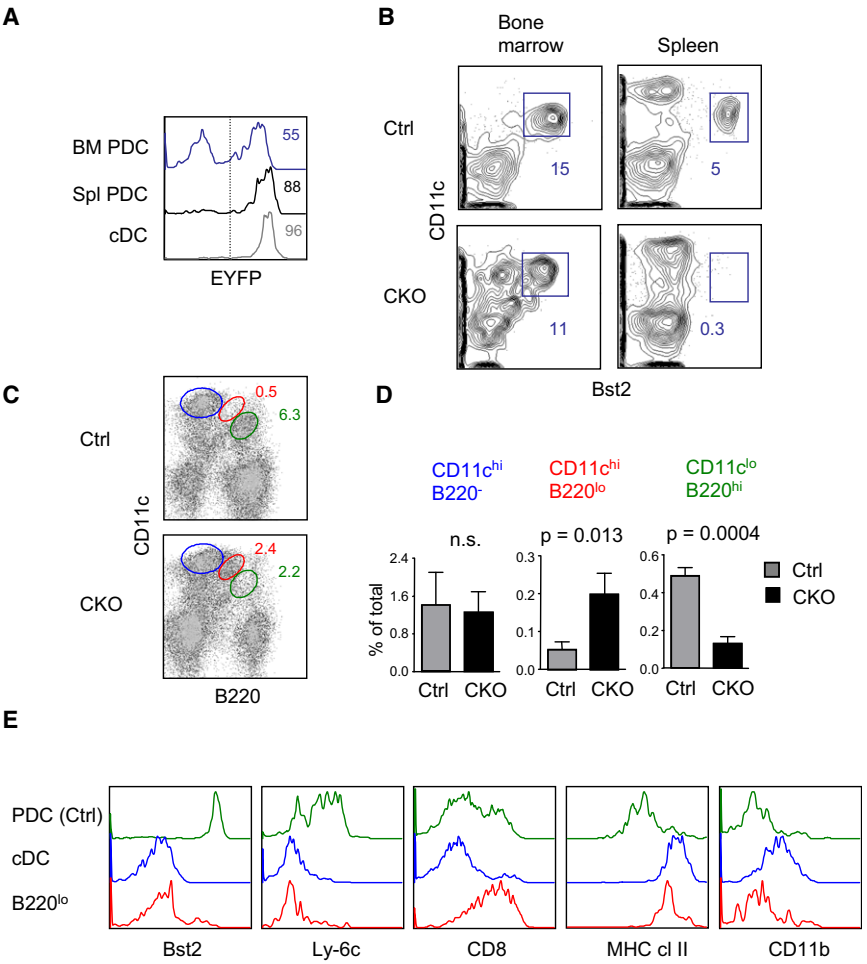

Figure 1. E2-2 Deletion in the Periphery Causes Spontaneous pDC Differentiation

(A) Recombination efficiency in the pDCs from *Itgax*-Cre deleter strain, as measured by Cre-inducible EYFP reporter expression in *Itgax*-Cre$^+$ *Gt(ROSA)26Sor*-EYFP$^+$ mice. Shown are representative histograms of EYFP fluorescence in gated CD11c^{lo} Bst2$^+$ pDCs from the BM or spleen and in splenic CD11c^{hi} MHC II$^+$ cDCs as a control. The positive threshold of EYFP fluorescence is indicated by a dashed line.

(B) The pDC population within Cre reporter-positive cells in the *Gt(ROSA)26Sor*-EYFP$^+$ *Itgax*-Cre$^+$ *Tcf4*$^{flox/-}$ conditional knockout (CKO) or *Gt(ROSA)26Sor*-EYFP$^+$ *Itgax*-Cre$^+$ control (Ctrl) mice. Shown are staining profiles of EYFP$^+$ cells in the BM or spleen, with the fraction of CD11c^{lo} Bst2$^+$ pDCs indicated.

(C) DC populations within Cre reporter-positive splenocytes in control and CKO mice. Shown are staining profiles of EYFP$^+$ cells; highlighted are CD11c^{hi} B220$^-$ cDCs (blue), CD11c^{lo} B220$^+$ pDCs (green), and the CD11c^{hi} B220^{lo} cDC-like population (red).

(D) The fraction among total splenocytes of the cell populations shown above (mean ± SD of three animals per genotype). n.s., not significant.

(E) Cell surface phenotype of the B220^{lo} cDC-like population. Shown are staining histograms of EYFP$^+$ splenocyte populations shown in (C), including pDCs from control mice and cDCs and the B220^{lo} cDC-like cells from CKO mice. Representative of three CKO animals.

murine *Dntt* and *Ccr9* (Reizis, 2010). Thus, the lineage identity of pDCs remains controversial, and their relationship to cDCs requires further genetic evidence.

Recently, we have shown that class I basic helix-loop-helix transcription factor (E protein) E2-2 (official symbol Tcf4) is a critical regulator of pDC lineage specification in mice and in humans (Cisse et al., 2008). E proteins are important regulators of lymphopoiesis, with other family members E2a and HEB controlling the development of B and T lymphocytes, respectively (D'Cruz et al., 2010; Kee, 2009). The activity of E proteins is antagonized by Id family transcription factors such as Id2, which prevent E protein binding to DNA. Murine and human mature pDCs express high E2-2 but low levels of Id2, whose overexpression blocks pDC development (Cisse et al., 2008; Nagasawa et al., 2008; Spits et al., 2000). E2-2-deficient hematopoietic cells cannot give rise to pDCs, whereas pDCs from mice and from human patients heterozygous for E2-2 manifest aberrant surface phenotype and defective IFN secretion (Cisse et al., 2008). In particular, murine *Tcf4*$^{+/-}$ pDCs show reduced expression of the genes that are specific for pDCs (*Irf7*) or shared between pDCs and lymphocytes (*Dntt*, *Ccr9*, *Spib*).

Based on these results, we hypothesized that E2-2 expression diverts pDCs from the common DC developmental pathway and imparts them with "lymphoid" features (Reizis, 2010). In this scenario, the resulting pDC fate can be either irreversibly "locked" by epigenetic mechanisms or actively enforced by the presence of E2-2. To test these possibilities, we analyzed the consequences of constitutive or inducible loss of E2-2 in the peripheral pDCs in vivo. We now report that E2-2-deficient mature pDCs spontaneously acquire phenotypic, morphological, and functional properties of cDCs. Furthermore, we provide evidence that E2-2 directly activates pDC-specific gene expression program and might repress genes associated with the alternative cDC lineage. Therefore, continuous E2-2 expression in mature pDCs is required to maintain their unique lineage identity and antagonize the "default" cDC cell fate.

RESULTS

Constitutive Deletion of E2-2 in Peripheral pDCs Generates a cDC-like Population

To test the role of E2-2 in pDC maintenance, we performed stage-specific recombination of the conditional *Tcf4* allele (*Tcf4*^{flox}) in mature peripheral pDCs. To this end, we used the *Itgax*-Cre (also known as *CD11c*-Cre) deleter strain, in which recombination occurs in 50%–60% of BM pDCs but increases to ~90% in splenic pDCs (Figure 1A; Caton et al., 2007). To increase the frequency and visibility of pDCs that underwent

Cre recombination, we have combined a conditional and a germline null *Tcf4* alleles and introduced Cre-inducible enhanced yellow fluorescent protein reporter allele (*Gt(ROSA)26Sor*-EYFP). In the resulting *Itgax*-Cre^{+} *Tcf4*$^{flox/-}$ *Gt(ROSA)26Sor*-EYFP^{+} conditional deletion mice, EYFP^{+} pDCs were readily detectable in the BM but completely absent from the spleen (Figure 1B), suggesting that some pDCs develop but do not persist in the periphery. Notably, the analysis of splenic EYFP^{+} cells revealed a new CD11c^{hi}B220^{lo} population appearing as an intermediate between pDCs and cDCs (Figures 1C and 1D). These cells lacked pDC markers Bst2 and Ly-6c but expressed high levels of MHC II and CD8, consistent with the cDC phenotype (Figure 1E).

We also analyzed fully conditional *Itgax*-Cre^{+} *Tcf4*$^{flox/flox}$ mice, which demonstrate a partial deletion of splenic pDCs (Cisse et al., 2008). Although less conspicuous without a Cre reporter, the same CD11c^{hi}B220^{lo} MHC II^{+} Bst2^{-} population was markedly elevated in the *Itgax*-Cre^{+} *Tcf4*$^{flox/flox}$ spleens (Figure S1 available online). On the other hand, this population was not observed in the animals reconstituted with *Tcf4*$^{-/-}$ hematopoietic progenitors, in which pDC development in the BM is completely blocked (data not shown). Therefore, this population probably represents the progeny of pDCs that escape early E2-2 deletion in the BM and lose E2-2 only in the periphery. These data suggest that the loss of E2-2 in peripheral pDCs causes their spontaneous differentiation into cells with cDC phenotype.

Inducible Deletion of E2-2 in pDCs Causes Acquisition of cDC Phenotype

To analyze the fate of mature pDCs after E2-2 deletion, we used *Gt(ROSA)26Sor*-CreER deleter mice that express tamoxifen (Tmx)-inducible Cre recombinase. High-dose Tmx administration to *Gt(ROSA)26Sor*-CreER^{+} *Tcf4*$^{flox/flox}$ mice leads to rapid pDC loss (Cisse et al., 2008). After the induction with a lower dose of Tmx, splenic pDCs were present in normal numbers at days 2–4 but largely disappeared by day 9 (data not shown). Because pDCs are relatively long lived, we hypothesized that such rapid depletion may be caused by a defect in peripheral pDCs. We therefore analyzed E2-2-deficient splenic pDCs on day 6 after Tmx treatment, when pDC numbers were reduced by ~50% (Figure 2A). Notably, pDC survival at this stage was not impaired (Figure S2), suggesting that pDCs may undergo phenotypic conversion rather than cell death.

To test whether acute E2-2 loss depletes pre-existing mature pDCs, *Gt(ROSA)26Sor*-CreER^{+} *Tcf4*$^{flox/flox}$ mice were fed with nucleoside analog bromodeoxyuridine (BrdU) for 2 weeks ("pulse"), followed by BrdU withdrawal ("chase") at the start of Tmx treatment. In contrast to the CD8^{+} cDCs that largely turned over after 8 days of chase (corresponding to day 6 after Tmx treatment), a substantial fraction of pDCs retained BrdU (Figure 2B). Notably, both BrdU^{+} (i.e., pre-existing) and BrdU^{-} (i.e., newly generated) splenic pDCs were reduced in *Gt(ROSA)26Sor*-CreER^{+} *Tcf4*$^{flox/flox}$ mice at that point (Figure 2C). Furthermore, the analysis of CD8^{+} cDCs in CKO spleens revealed a novel B220^{+} population that was ~50% BrdU^{+} (Figure 2D). Because cDCs do not express E2-2 (Cisse et al., 2008) and their proliferation was not changed by E2-2 deletion (Figure S2), the B220^{+} BrdU^{+} cDCs may have developed from pre-existing B220^{+} cells such as pDCs. Thus, the induction of E2-2 loss from mature splenic pDCs leads to their depletion, probably through differentiation into B220^{+} cells with CD8^{+} cDC phenotype.

To trace the fate of splenic pDCs after induced E2-2 deletion, we used human pre-T cell receptor α (*PTCRA*) transgenic mice that express enhanced green fluorescent protein (EGFP) specifically in pDCs (Shigematsu et al., 2004). Because EGFP protein is very stable without cell division and marks immediate progeny of EGFP^{+} cells (Boursalian et al., 2004), *PTCRA*-EGFP expression facilitates the tracing of pDC progeny. In control *PTCRA*-EGFP^{+} animals 6 days after Tmx treatment, splenic B220^{+} EGFP^{+} pDCs were uniformly Bst2^{+} CD11c^{lo} MHC II^{lo} (Figure 2E). In contrast, >30% of B220^{+} EGFP^{+} splenocytes in Tmx-treated *PTCRA*-EGFP^{+} *Gt(ROSA)26Sor*-CreER^{+} *Tcf4*$^{flox/flox}$ animals lost Bst2 expression; this Bst2^{-} pDC fraction showed a particularly strong upregulation of CD11c and MHC II nearly to the level of cDCs. Furthermore, B220^{+} EGFP^{+} E2-2-deficient cells downregulated CCR9 and Ly-6c and upregulated CD8 in a larger fraction of cells (Figure 2F and data not shown). The increase in MHC II occurred in both CD8^{lo} and CD8^{hi} pDC populations (data not shown), suggesting that it is independent of the heterogeneous CD8 expression on pDCs.

To test whether similar phenotypic conversion may be observed in vitro, E2-2 deletion was induced in Flt3L-supplemented BM cultures. The expansion of CD11c^{hi} cDC-like cells at the expense of pDCs was observed as early as 2 days after Tmx addition to *PTCRA*-EGFP^{+} *Gt(ROSA)26Sor*-CreER^{+} *Tcf4*$^{flox/flox}$ cultures (Figure S2). The rapid phenotypic changes suggest that E2-2 protein levels closely follow the transcript levels after deletion. Altogether, these data demonstrate that acute loss of E2-2 from mature pDCs causes their spontaneous conversion into cDC-like cells.

In view of these results, we tested whether pDC abnormalities in *Tcf4*$^{+/-}$ mice (Cisse et al., 2008) could be intrinsic to peripheral pDCs. Indeed, *Tcf4*$^{+/-}$ pDCs showed increased expression of CD8, CD11c, and MHC II only in the spleen, not in the BM (data not shown). Furthermore, in *PTCRA*-EGFP^{+} *Tcf4*$^{+/-}$ mice, EGFP^{+} pDCs upregulated CD11c and MHC II expression (Figure S2), as observed after E2-2 deletion (Figure 2E). Thus, peripheral pDCs in *Tcf4*$^{+/-}$ mice spontaneously upregulate cDC markers, suggesting that reduced E2-2 expression causes phenotypic conversion to cDC-like cells.

E2-2-Deficient pDCs Acquire cDC Properties

To analyze the morphology of pDCs after acute E2-2 loss, sorted EGFP^{+} pDCs from Tmx-treated *PTCRA*-EGFP^{+} control and *Gt(ROSA)26Sor*-CreER^{+} *Tcf4*$^{flox/flox}$ mice were stained for actin cytoskeleton. As shown in Figure 3A, the majority (72%) of control pDCs had a characteristic round perinuclear actin staining; the remaining cells showed only minimal changes of cell shape or actin cytoskeleton, and none had dendrites. In contrast, 67% of E2-2-deficient pDCs showed irregular shape and/or prominent actin remodeling, and 17% had overt dendrites similar to those of cDCs (Figures 3A and 3B).

Next, we tested the Ag presentation capacity of E2-2-deficient pDCs. Consistent with their low MHC II expression, unstimulated splenic pDCs cannot prime CD4^{+} T cell responses (Young et al., 2008). Indeed, sorted CD11c^{lo} EGFP^{+} pDCs from control *PTCRA*-EGFP^{+} animals failed to induce proliferation of naive

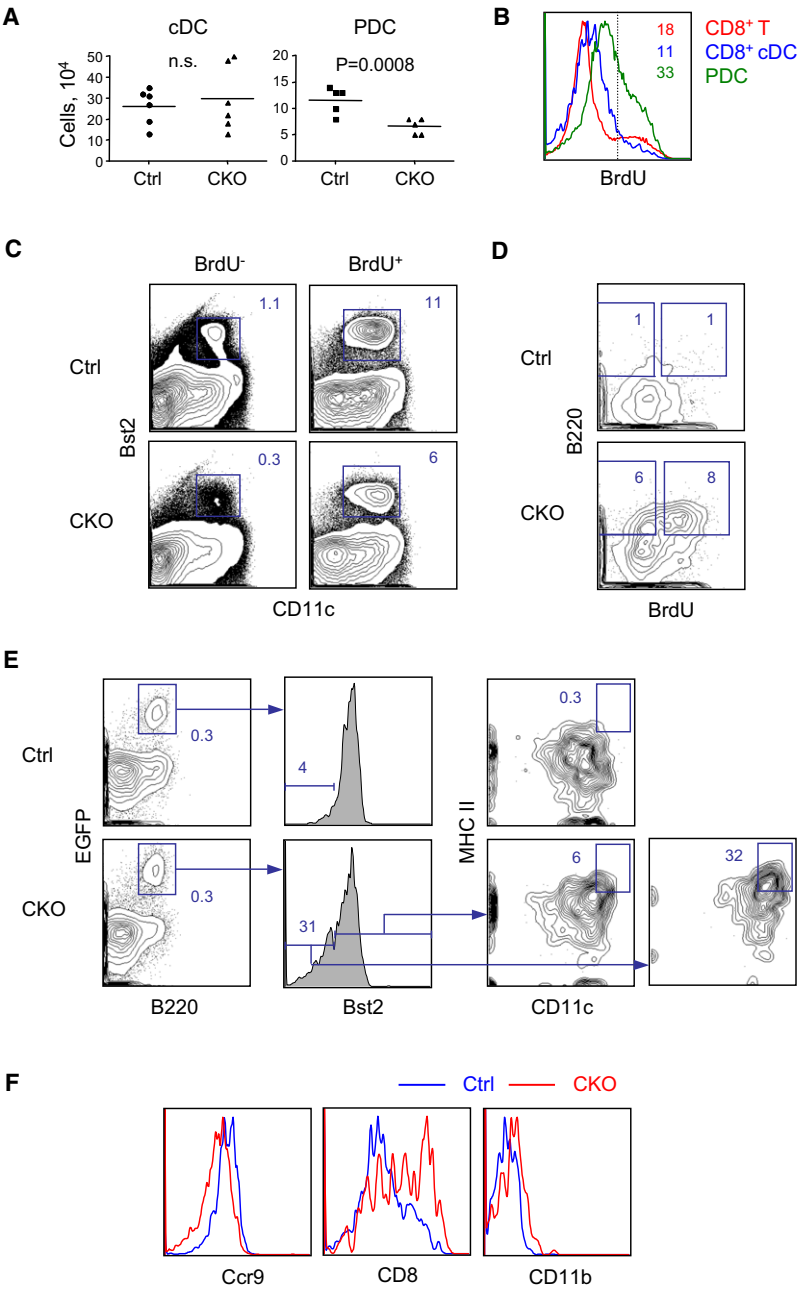

Figure 2. Inducible Loss of E2-2 in Mature pDCs Causes Differentiation into cDC-like Cells

(A) Reduction of PDC numbers shortly after E2-2 deletion. Tamoxifen (Tmx)-inducible *Gt(ROSA)26Sor*-CreER$^+$ *Tcf4*$^{flox/flox}$ CKO mice or Cre-negative littermate controls (Ctrl) were treated with Tmx and analyzed on day 6 after the last administration. Shown are absolute numbers of splenic cDC (CD11c^{hi} MHC II$^+$) and PDC (CD11c^{lo} Bst2$^+$) in the individual CKO and control mice. n.s., not significant.

(B) BrdU labeling of pre-existing pDCs. Tmx-inducible CKO and control mice were kept on BrdU for 14 days, followed by simultaneous 3 day Tmx treatment and BrdU withdrawal for 8 days. Shown is BrdU incorporation in the splenic CD8$^+$ T cells, CD8$^+$ CD11c^{hi} cDCs, or CD11c^{lo} Bst2$^+$ pDCs from control mice. The threshold of high-level BrdU staining is indicated by the dashed line.

(C) The fraction of pDCs among BrdU^{hi} or BrdU$^-$ splenocytes pooled from 3–4 control and CKO animals.

(D) BrdU incorporation and B220 expression in the splenic CD8$^+$ CD11c^{hi} MHC II$^+$ cDCs from control and CKO mice. The percentages of B220$^+$ BrdU$^-$ and B220$^+$ BrdU$^+$ cells are indicated.

(E) Cell surface phenotype of pDCs after Tmx-induced E2-2 deletion in *PTCRA*-EGFP reporter mice. Conditional *PTCRA*-EGFP$^+$ *Gt(ROSA)26Sor*-CreER$^+$ *Tcf4*$^{flox/flox}$ (CKO) mice or Cre-negative littermate controls (Ctrl) were treated with Tmx and analyzed 6 days later. Shown are the fractions among total splenocytes and the staining profiles of B220$^+$ EGFP$^+$ pDCs, with the CD11c^{hi} MHC II$^+$ cDC gate indicated. Whereas the fraction of EGFP$^+$ pDCs was variable because of partial EGFP expression in pDCs (Shigematsu et al., 2004), their phenotypic changes are representative of >5 CKO animals.

(F) Staining histograms of gated B220$^+$ EGFP$^+$ pDCs from CKO and control mice (representative of three independent experiments).

allogeneic CD4$^+$ T cells (Figure 3C). In contrast, CD11c^{lo} EGFP$^+$ pDCs from Tmx-treated *Gt(ROSA)26Sor*-CreER$^+$ *Tcf4*$^{flox/flox}$ mice induced a significant allogeneic response. A similar increase in T cell proliferation was observed in ovalbumin-specific priming of TCR transgenic CD4$^+$ T cells by E2-2-deficient pDCs from ovalbumin-pulsed animals (data not shown). Thus, E2-2-deficient peripheral pDCs acquire dendritic morphology and capacity for CD4$^+$ T cell priming, the salient features of cDCs.

E2-2-Deficient pDCs Upregulate cDC-Associated Genes

To characterize gene expression changes underlying the observed phenotypic and morphological conversion, we examined global expression profile of peripheral pDCs after E2-2 deletion. Control and *Gt(ROSA)26Sor*-CreER$^+$ *Tcf4*$^{flox/flox}$ animals were treated with Tmx, and CD11c^{lo} Bst2$^+$ pDCs were sorted on days 4 or 6 and analyzed by Affymetrix expression microarrays. The rigorous definition of pDCs as Bst2$^+$ and the additional 4 day time point were used to focus on the earliest and most reliable changes of gene expression. Principal component analysis (PCA) was used to define probe sets that were coordinately induced or decreased in CKO pDCs at both time points (60 and 70 probes, respectively, out of 24,505 total probes; Figure 4A; Table S1). The upregulated set included three probes for *Cd8a*, consistent with CD8 upregulation in E2-2-deficient pDCs (Table 1). Furthermore, many of the upregulated (16/60) and downregulated (14/70) probes were correspondingly changed in the previous microarray analysis of *Tcf4*$^{+/-}$ pDCs (Table 1; Table S1).

Next, we used PCA to analyze normal expression profiles of the differentially expressed genes. No clear pattern could be established among the downregulated genes, although several of these (*Matn2, Fcrla, Sla2, Notch3*) are prominently enriched in pDCs. In contrast, the upregulated genes comprised two principal components: enriched in cDCs (16/60 probes) and

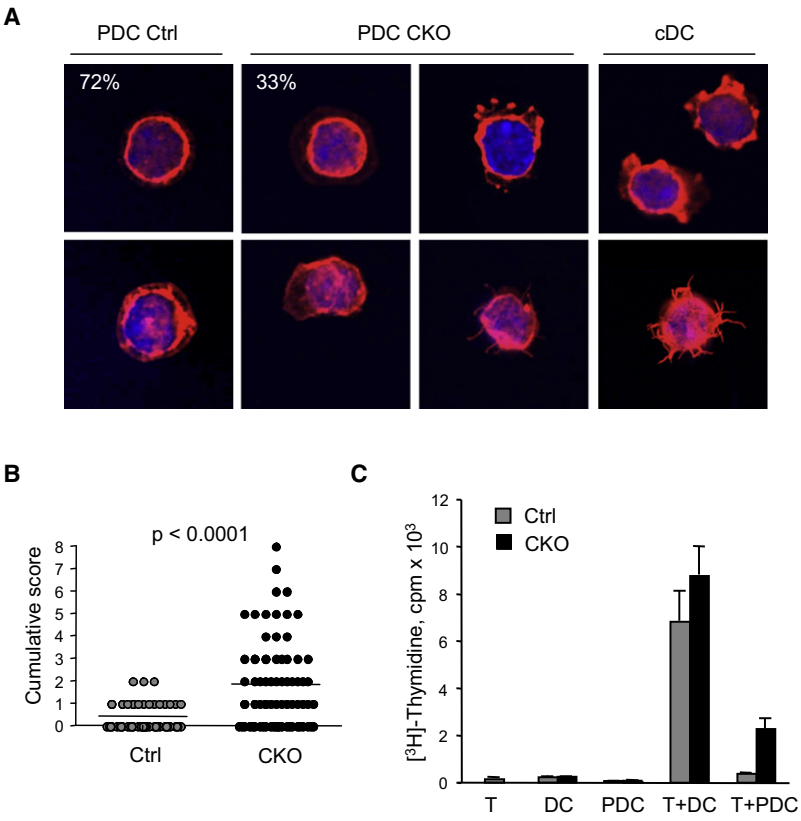

Figure 3. E2-2-Deficient pDCs Acquire Morphological and Functional Properties of cDCs

Conditional *PTCRA*-EGFP$^+$ *Gt(ROSA)26Sor*-CreER$^+$ *Tcf4*$^{flox/flox}$ (CKO) mice or Cre-negative littermate controls (Ctrl) were treated with Tmx, and 6–7 days later splenic EGFP$^+$ CD11c$^{lo/int}$ pDCs and EGFP$^-$ CD11c^{hi} cDCs were isolated by flow cytometry.

(A) Representative confocal photomicrographs of pDCs stained for actin cytoskeleton (phalloidin, red) and nuclear DNA (DAPI, blue). For control cells, the typical pDC morphology (72% of all cells) and the most extreme example of actin remodeling are shown. For CKO cells, the examples of pDC morphology (33% of all cells), actin remodeling, and dendrites are shown, along with sorted cDCs as a positive control.

(B) Quantitative analysis of pDC morphology. Confocal microscopy images shown in (A) were scored for irregular cell shape, actin cytoskeleton remodeling, and dendrites, and cumulative scores of individual control (n = 55) and CKO (n = 75) cells are shown.

(C) T cell priming capacity of pDCs. The pDCs or cDCs were sorted as above and cultured alone or with purified allogeneic CD4$^+$ T cells, and thymidine incorporation was determined 72 hr later (mean ± SD of triplicate cultures).

enriched in cDCs and B cells (9/60 probes) (Figure 4B). Moreover, seven of the upregulated genes belong to the evolutionarily conserved signature that distinguishes cDCs from pDCs (Table 1; Table S1; Robbins et al., 2008). Despite the induction of CD8, a substantial fraction of the upregulated genes (14/60) is characteristic of the CD8$^-$ rather than CD8$^+$ cDC subset (Figure 4C; Table S1). Thus, the resulting CD8$^+$ cDC-like cells appear distinct from the bona fide CD8$^+$ cDCs and instead may resemble the recently described CD8-expressing cDC subset related to CD8$^-$ cDCs and pDCs (Bar-On et al., 2010). Functionally, several upregulated genes (*Fscn1, Pak1, Dock4*) control cytoskeletal organization, including Fscn1 as a known regulator of cDC morphology (Al-Alwan et al., 2001). Furthermore, MHC II presentation pathway genes (*H2-DMb2, H2-Ob*) were induced, consistent with the acquisition of cDC properties and the corresponding morphological and functional switch.

Next, cDCs and pDCs independently sorted from *Gt(ROSA)26Sor*-CreER$^+$ *Tcf4*$^{flox/flox}$ mice 5 days after Tmx treatment were analyzed by quantitative RT-PCR (qPCR). This analysis confirmed microarray results and expression patterns in pDCs and cDCs for the relevant differentially expressed genes (Table 1; Figure 4D). In addition, CKO pDCs showed downregulation of pDC-enriched transcription factors *Spib* and *Bcl11a* and induction of *Id2* and *CIITA* isoform *pI*, both of which are highly enriched in cDCs compared to pDCs (Figure 4D). The downregulation of *Bcl11a* after E2-2 deletion was confirmed in BM-derived pDC cultures (Figure S3). Overall, the changes of transcription factor profile are consistent with the onset of conversion to cDC-like cells by E2-2-deficient pDCs.

E2-2 Directly Controls the Expression Program of pDCs

The data so far indicate that E2-2 maintains pDC cell fate and prevents spontaneous conversion into cDC-like cells. To test whether E2-2 mediates these effects through direct binding to the relevant genes, we performed chromatin immunoprecipitation followed by genome-wide promoter microarray hybridization (ChIP-on-chip) in the human pDC cell line CAL-1. The resulting probabilities of probe binding (pXbar) by E2-2-associated chromatin yielded binding profiles of E2-2 across the 5′ regions of genes (Figures 5A and 5B). By using stringent criteria (pXbar < 0.01, pXbar ratio of E2-2 and control ChIP < 0.1), we have defined high-confidence list of 2,477 genes (corresponding to 4,369 probes, out of ~17,000 genes and 474,392 probes total) as E2-2 binding targets (Table S2). The list included several genes reduced in murine E2-2-deficient and/or *Tcf4*$^{+/-}$ pDCs (*SPIB, IRF7, FCRLA, SLA2, DNTT*), suggesting these genes as conserved E2-2 targets (Table 2). Notably, the target list included 20 of 55 (36%) human pDC-specific genes compared to 6 of 47 (13%) genes expressed in both pDCs and myeloid cells; furthermore, 23% of conserved pDC "signature" genes (Robbins et al., 2008) represented E2-2 binding targets (Table S3). Indeed, several uniquely pDC-specific genes such as *LILRA4* (encoding ILT7; Cao et al., 2006), *PACSIN1* (Robbins et al., 2008), and *CD2AP* (Marafioti et al., 2008) were strongly bound by E2-2 (Table 2; Figure 5A). Moreover, E2-2 binding targets (Table 2) included key functional genes in pDCs such as transcription factors (*SPIB, IRF7, CIITA pIII*), components of TLR signaling pathway (*TLR9, TLR7-TLR8, UNC93B1, BTK*), and BCR-like signaling cascade that inhibits IFN response (*TYROBP, PIK3AP1, BLNK*) (Gilliet et al., 2008). These data suggest that E2-2 directly controls the specific gene expression program of mature pDCs.

In addition to pDC-specific genes, E2-2 target list included genes associated with the alternative cDC fate, such as *ITGAX*

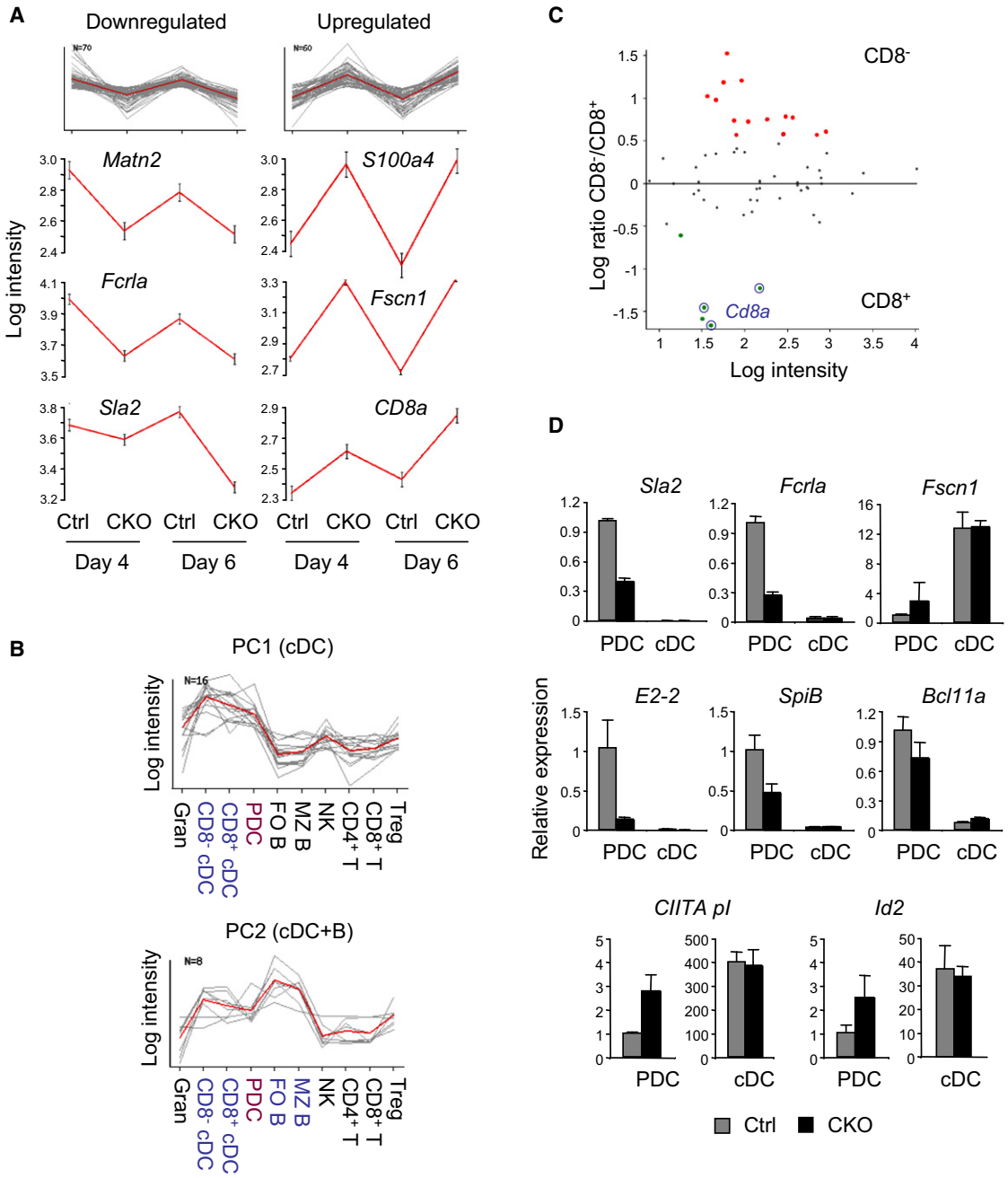

Figure 4. E2-2-Deficient pDCs Upregulate cDC-Enriched Genes

(A) Genes coordinately changed in pDCs on days 4 and 6 after E2-2 deletion. The pDCs were sorted from *Gt(ROSA)26Sor*-CreER^{+} *Tcf4*$^{flox/flox}$ (CKO) mice or littermate controls 4 and 6 days after Tmx treatment and subjected to genome-wide expression profiling via microarrays. Principal component analysis (PCA) was used to identify probes up- or downregulated in CKO samples on both days. Top panels show expression graphs of individual probes (gray) and the principal component (red); lower panels show expression graphs for the indicated representative probes. Data represent log hybridization intensity of probes (average ± SD of duplicate array samples).

(B) Expression profile of the genes upregulated in E2-2-deficient pDCs. For the 60 probes upregulated in pDCs after E2-2 deletion, normal expression values in major immune cell types were derived from GEO data set GSE9810 and subjected to PCA. Shown are expression graphs for the two major principal components (cDC-enriched and cDC+B cell-enriched probes).

(C) The cDC subset specificity of the upregulated genes. The 60 probes upregulated in pDCs after E2-2 deletion were queried for their expression in the normal CD8^{-} and CD8^{+} cDC subsets (GEO data set GSE9810). Shown is log-ratio plot comparison of expression values in CD8^{-} and CD8^{+} cDCs, with the probes overexpressed >3-fold highlighted in red and green, respectively. The three probes for *Cd8a* are circled.

(D) Quantitative analysis of gene expression in E2-2-deficient pDCs. The pDCs (CD11c^{lo} Bst2^{+}) and cDCs (CD11c^{hi} Bst2^{-}) were sorted from control and CKO animals 5 days after Tmx treatment and analyzed by qRT-PCR for microarray target genes (top row) and downregulated (middle row) and upregulated (bottom row) transcription factors. Data represent normalized expression values relative to the control pDC sample (mean ± SD of triplicate reactions).

Table 1. Differentially Expressed Genes in E2-2-Deficient pDCs

Gene	Probe	Fold Change	Fold Change (qPCR)	*Tcf4*$^{+/-}$ PDC	Expression Pattern (PCA)	Expression Signature	E2-2 ChIP Target
Reduced							
Notch3	1421965_s_at	2.3	n.d.	down			
Fcrla	1419907_s_at	2.1	3.8	down		pDC	yes
Matn2	1455978_a_at	2.3	2.2	down			
Sla2	1437504_at	2.3	2.6			pDC	yes
Increased							
Cd8a	1444078_at, 1425335_at, 1440811_x_at	2.5	n.d.	up			
H2-DMb2	1443686_at, 1443687_x_at	2.6	2.9	up	cDC+B		yes
H2-Ob	1440837_at	2.4	4.1	up	cDC+B	cDC	
Fscn1	1416514_a_at	4.1	2.9		cDC	cDC	
S100a4	1424542_at	4.8	4.3	up		CD8$^-$ cDC	
Pak1	1450070_s_at	2.7	1.8		cDC	cDC	
Hspa1b	1427126_at	2.1	n.d.	up	cDC		
Tmem176a	1441811_x_at	4.0	1.7		cDC		yes
1100001H23Rik	1448786_at	2.4	1.9	up	cDC	cDC	

Sorted pDCs were analyzed by expression microarrays 4 or 6 days after Tmx-induced E2-2 deletion, and genes coordinately increased or reduced in E2-2-deficient compared to control pDCs were defined (Table S1). Shown are select target genes with the corresponding microarray probes; average fold change by microarray analysis; fold change determined by qRT-PCR in independently sorted pDCs on day 5 after Tmx treatment; >2-fold change, if any, in pDCs from *Tcf4*$^{+/-}$ mice heterozygous for E2-2 (Cisse et al., 2008); expression pattern as determined by PCA of normal expression values in GSE9810; conserved "expression signature" (Robbins et al., 2008); and high-confidence E2-2 binding in human pDCs as determined by ChIP-on-ChIP (Table S2). n.d., not done.

and *HLA-DMA* (12.5% of conserved cDC "signature" genes) (Robbins et al., 2008). Furthermore, cDC-enriched genes induced in E2-2-deficient pDCs such as *HLA-DMB, S100A4*, *TMEM176A*, and *ID2* were specifically bound by E2-2 (Figure 5B; Table S1). Thus, E2-2 may antagonize cDC cell fate in part by directly binding to and repressing cDC-associated genes.

DISCUSSION

Here we demonstrate that the reduction or loss of transcription factor E2-2 from mature pDCs caused their differentiation into cDC-like cells. In *Tcf4*$^{+/-}$ animals, peripheral pDCs showed increased expression of cDC markers and MHC II, indicating a "drift" toward cDC-like phenotype. This explains the reduced pDC-specific gene expression and IFN secretion capacity in murine and human *Tcf4*$^{+/-}$ pDCs (Cisse et al., 2008) and suggests that the haploinsufficiency of E2-2 is primarily due to the defective maintenance of peripheral pDCs. The deletion of E2-2 from mature pDCs via constitutive stage-specific or inducible deletion systems resulted in the appearance of a CD8$^+$ cDC-like population that retained some pDC markers such as B220 and *PTCRA*-EGFP. Further analysis of pDCs shortly after E2-2 deletion confirmed the acquisition of morphological and functional properties of cDCs and the induction of cDC gene expression program. Because cDCs are very short lived compared to pDCs, such differentiation accounts for the rapid disappearance of pDCs after E2-2 deletion. Overall, these data suggest that continuous expression of E2-2 is required to maintain the cell fate of mature pDCs and to prevent spontaneous cell fate conversion and eventual loss.

A major implication of the observed pDC conversion into cDC-like cells is that pDCs are genetically closer to cDCs than to any other lineage. The question of pDC origin and lineage identity has been highly controversial ever since the identification of pDCs as a separate cell type. Whereas common BM progenitors and dependence on Flt3 signaling suggest a close relationship with cDCs, pDCs show evidence of lymphoid origin such as D→J rearrangement of *IgH* and *TCRb* loci and history of *Rag1* expression (Corcoran et al., 2003; Pelayo et al., 2005; Welner et al., 2009). Indeed, in almost every aspect of morphology and physiology, pDCs resemble lymphocytes (particularly B cells) more than cDCs. To explain this apparent paradox, we proposed that pDCs are genetically and developmentally related to cDCs more than to any other lineage; however, the induction of E2-2 and the ensuing E protein-dependent gene expression program impart the unique lymphoid features upon pDCs (Reizis, 2010). Thus, the cDC cell fate may represent the "default" differentiation pathway of common DC progenitors, which is antagonized by E2-2 to specify pDC lineage. Our current results strongly support this model and extend it to demonstrate active repression of the "default" cDC cell fate by E2-2.

Although E2-2-deficient pDCs upregulate CD8α, they do not seem to differentiate into the bona fide CD8$^+$ cDCs. Indeed, CD8$^+$ cDC-specific genes such as *Tlr3*, *Xcr1*, or *Itgae* were not increased (data not shown), whereas many CD8$^-$ cDC-enriched genes became upregulated. Notably, a similar CD8$^+$ cDC population whose expression profile is related to CD8$^-$ cDCs and pDCs was recently identified in the lymphoid organs of naive mice via the *Cx3cr1*-EGFP reporter allele (Bar-On et al., 2010).

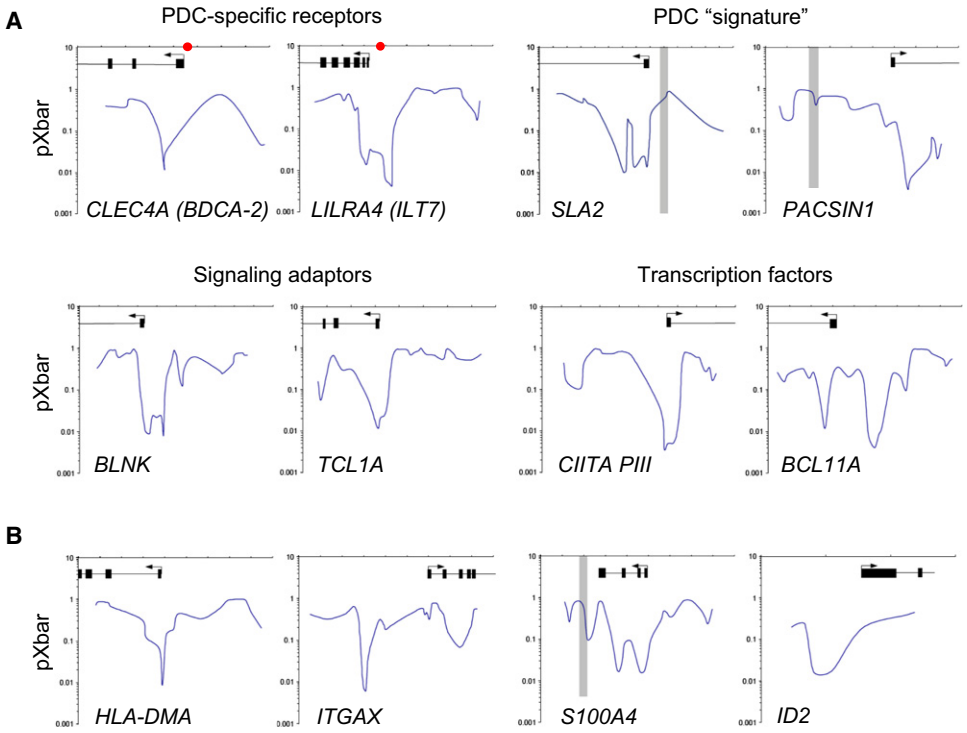

Figure 5. Direct Binding of E2-2 to Target Genes in pDCs

(A) The binding of E2-2 to the 5′ regions of pDC-specific target genes in the human pDC cell line CAL-1. Chromatin immunoprecipitated with anti-E2-2 or control antibodies was labeled and hybridized to a microarray containing ~10 kb promoter regions of ~17,000 human genes. Shown are graphs of E2-2 binding probability (pXbar) over the 5′ gene regions, highlighting exons (filled boxes) and transcription start sites (arrows). Horizontal axis divisions correspond to 1 kb. Regions showing high background binding in control antibody hybridization (pXbar < 0.1) are shaded in gray. Red dots represent the regions of binding determined by qPCR of unamplified chromatin (Cisse et al., 2008).

(B) The binding of E2-2 to the 5′ regions of cDC-enriched target genes in CAL-1, shown as above.

In particular, several genes upregulated in E2-2-deficient pDCs such as *S100a4* and *Trem176a* are prominently expressed in the Cx3cr1-EGFP$^+$ but not in the classical CD8$^+$ cDCs. Moreover, *Cx3cr1*-EGFP$^+$ CD8$^+$ cDCs express low E2-2 but require E2-2 expression in the BM for their development, suggesting that they arise from committed pDC progenitors that downregulate E2-2. Thus, the loss of E2-2 from mature pDCs and ''abortive'' pDC development in the steady state yield similar CD8$^+$ cDC subsets, which probably represent a common ''default'' fate of E2-2-deficient pDCs.

Human pDCs were first identified as efficient precursors of cDCs in the peripheral blood (Grouard et al., 1997), as shown by the fact that they acquire functional and morphological cDC properties when cultured in vitro with TLR ligands and/or cytokines (Soumelis and Liu, 2006). On the other hand, virus-induced conversion of pDCs to CD8$^-$ cDCs was observed only in the BM but not in the spleen, suggesting that mature pDCs in vivo have lost this capacity (Zuniga et al., 2004). Notably, however, in vitro activated pDCs reduce E2-2 expression by ~75% after 2 days, consistent with the loss of pDC lineage identity (Cisse et al., 2008); furthermore, many E2-2 target genes such as *Matn2* and *Fcrla* are prominently downregulated in activated pDCs (microarray data in Iparraguirre et al., 2008). Our observations suggest that E2-2 downregulation may play an active role after virus-induced pDC activation, e.g., by allowing pDC conversion into cDC-like cells and/or limiting IFN secretion. This hypothesis will be tested once a robust in vivo model of activation-induced pDC differentiation becomes available.

E2-2 is likely to maintain the cell fate of pDCs and oppose that of cDCs through several mechanisms. First, E2-2 binds to a large fraction of pDC-enriched genes by ChIP, including the key transcription factors and functional components of TLR signaling pathway and of inhibitory receptor signaling. These genes appear to be directly activated by E2-2, thereby contributing to pDC gene expression program and functionality. Second, direct targets of E2-2 may include pDC-specific transcriptional repressors that negatively regulate cDC-enriched genes. One attractive candidate is Bcl11a, a transcription factor that is highly expressed in murine and human pDCs and B cells (Marafioti et al., 2008; Pelayo et al., 2005). Moreover, Bcl11a is required for the development of B cells (Liu et al., 2003) as well as of pDCs (P. Tucker, personal communication). We found that human *BCL11A* promoter is a prominent E2-2 binding target and that murine *Bcl11a* expression is reduced after E2-2 deletion in pDCs. This is consistent with the recent identification of *Bcl11a* as a major direct target of E protein E2a in B lymphocytes (Lin et al., 2010). Because Bcl11a is a bona fide transcriptional repressor, it may at least partially mediate the repression of cDC-associated gene expression by E2-2.

Table 2. Select Targets of E2-2 Binding in Human pDCs

Gene	No. Probes	Rank	P(Xbar) E2-2	P(Xbar) Ctrl	Notes
Pathogen Sensing					
ZBP1 (DAI)	2	10	0.002	0.9	
PYCARD (ASC)	3	152	0.003	0.6	
TLR9	8	172	0.003	0.7	IFN induction
TLR7-TLR8[a]	3	248	0.003	0.7	IFN induction
UNC93B1	8	16	0.002	0.1	IFN induction
Surface Receptors					
LILRA4 (ILT7)	3	418	0.004	0.7	IFN inhibition; pDC specific
FCRLA	3	1271	0.006	1.0	
Signal Transduction					
BTK	4	531	0.004	0.8	IFN induction
TYROBP (DAP12)	2	77	0.003	0.8	IFN inhibition
PIK3AP1 (BCAP)	2	128	0.003	0.9	IFN inhibition
BLNK	3	1766	0.008	0.9	IFN inhibition
Transcription Factors					
BCL11A	3	205	0.003	0.4	pDC, B cells
CIITA PIII	5	209	0.003	1.0	pDC, B cells
SPIB	5	1065	0.006	0.3	pDC, B cells
IRF7	2	453	0.004	0.3	IFN induction; pDC specific
Other PDC-Enriched					
PACSIN1	3	147	0.003	0.9	pDC specific
SLA2	1	2326	0.009	0.4	pDC enriched
CD2AP	4	686	0.005	0.3	pDC enriched
PTCRA	5	1295	0.006	0.5	pDC (human), immature lymphocytes
DNTT	4	178	0.003	0.7	pDC (mouse), immature lymphocytes
BST2	4	307	0.004	0.4	pDC specific (mouse)

ChIP-on-Chip with anti-E2-2 or control antibodies was performed in human pDC cell line CAL-1. Shown are select genes among the high-confidence list of E2-2 binding targets (Table S2), with the number of bound probes, rank of the highest signal probe, and binding probability P(Xbar) for E2-2 and control hybridizations. The TLR-mediated IFN induction pathway and pDC-specific IFN inhibitory pathway are reviewed in Gilliet et al. (2008). Expression profiles are derived from the published data (Robbins et al., 2008).
[a] Binding peak located in the genomic region between *TLR7* and *TLR8*.

In addition, E2-2 might directly repress at least certain cDC genes, as suggested by E2-2 binding to several such genes in a pDC cell line. This may be particularly relevant for the genes that are expressed in pDCs but at lower levels relative to cDCs, such as *Itgax* (encoding CD11c) and MHC class II pathway genes. Although E proteins primarily activate transcription, they are also capable of repression in some cases (Kee, 2009). Notably, one apparent target of E2-2-mediated repression is Id2, an antagonist of E proteins. Id2 is abundantly expressed in cDCs and is required for the development of certain cDC subsets such as Langerhans cells and $CD8^+$ cDCs (Hacker et al., 2003); conversely, its overexpression blocks pDC development in vitro (Spits et al., 2000). Thus, the reduction of E2-2 may initiate a feed-forward loop that further inhibits E2-2 through Id2 induction and amplifies the loss of pDC cell fate. These data suggest a dynamic control of pDC and cDC cell fate through the bidirectional inhibition between E2-2 and Id2.

Recent evidence suggests that ''terminal'' differentiation state of a cell is in fact reversible, as first demonstrated by direct genetic reprogramming of mature B lymphocytes into macrophages (Xie et al., 2004). Furthermore, differentiated state is often maintained by continuous expression of a single transcriptional ''master regulator,'' and its removal may cause transdifferentiation into a reciprocal cell fate. For instance, deletion of Pax5 from mature B cells leads to dedifferentiation into lymphoid progenitors that give rise to T cells (Cobaleda et al., 2007). Likewise, the loss of FoxP3 from mature regulatory T cells abolishes their maintenance and causes autoimmunity (Williams and Rudensky, 2007). Our work provides another example of a postmitotic, long-lived, highly specialized immune cell type whose identity is actively maintained and reversible. These results reveal a close genetic relationship between pDCs and cDCs and establish a model to elucidate their unique genetic programs and functions.

EXPERIMENTAL PROCEDURES

Animals

The *PTCRA*-EGFP (129/SvEvTac, 129) (Shigematsu et al., 2004), $Tcf4^{+/-}$ (129) (Zhuang et al., 1996), $Tcf4^{flox}$ (C57BL/6, B6) (Bergqvist et al., 2000), *Itgax*-Cre

(B6) (Caton et al., 2007), *Gt(ROSA)26Sor*-CreER (B6) (Cisse et al., 2008), and *Gt(ROSA)26Sor*-EYFP (mixed B6/129) (Srinivas et al., 2001) mouse strains were used or intercrossed as indicated. For BrdU incorporation, mice were injected with 1 mg BrdU i.p. and then maintained for 2 weeks on drinking water with 0.8 mg/mL BrdU (Sigma-Aldrich). For the induction of Cre recombination in *Gt(ROSA)26Sor*-CreER$^+$ mice, tamoxifen (Sigma) was administered orally for 3 consecutive days (1 mg in 0.1 ml sunflower oil per day). Because CreER induction per se does not affect pDC numbers or phenotype (Cisse et al., 2008), Cre-negative *Tcf4*$^{flox/flox}$ littermates were used as controls for *Tcf4*$^{flox/flox}$ *Gt(ROSA)26Sor*-CreER$^+$ animals. All animal studies were performed according to the investigator's protocol approved by the Institutional Animal Care and Use Committee of Columbia University.

Cell Analysis

Single-cell suspensions were stained for multicolor analysis with the indicated fluorochrome-conjugated antibodies (BD PharMingen or eBioscience). For analysis of *Gt(ROSA)26Sor*-CreER$^+$ animals, DCs and pDCs were enriched by negative selection against CD3$^+$ and CD19$^+$ lymphocytes via MACS columns (Miltenyi Biotech). The samples were acquired with the LSR II flow cytometer or sorted on FACSAria flow sorter (BD Biosciences) and analyzed with FlowJo software (TreeStar). For BrdU incorporation, cells from 3–4 pooled spleens were enriched for DCs and pDCs by negative selection, stained for surface markers, fixed, permeabilized, and stained with an antibody against BrdU according to the BD PharMingen BrdU Flow Kit protocol.

For cell morphology analysis, splenic pDCs (CD11c^{lo} EGFP$^+$) and cDCs (CD11c^{hi} EGFP$^-$) from *PTCRA*-EGFP$^+$ *Gt(ROSA)26Sor*-CreER$^+$ *Tcf4*$^{flox/flox}$ mice and Cre-negative littermate controls 7 days after Tmx treatment were sorted onto positively charged glass slides. Cells were fixed with 3% paraformaldehyde for 15 min at 37°C, washed in PBS, and incubated with 100 mM glycine for 10 min at room temperature. Fixed cells were lysed with 0.1% Triton X-100 for 4 min, washed with PBS, blocked with 1% BSA, and stained with Rhodamine-phalloidin (Cytoskeleton, Inc.) and DAPI. Images were acquired with LSM 710 NLO confocal microscope and ConfoCor 3 imager (Carl Zeiss). For semiquantitative analysis of cell morphology, images of individual pDCs in the same central plane were coded and scored by a blinded observer for three categories: irregular shape, actin rearrangement to cell periphery, and dendrites. Each category was scored from 0 (none) to 3 (maximal), and a cumulative score was derived for each cell.

T Cell Proliferation

Splenic CD11c$^+$ cells from *PTCRA*-EGFP$^+$ *Gt(ROSA)26Sor*-CreER$^+$ *Tcf4*$^{flox/flox}$ mice and Cre-negative littermate controls 7 days after Tmx treatment were enriched by positive selection via MACS columns (Miltenyi Biotech), and pDCs (CD11c^{lo} EGFP$^+$) and cDCs (CD11c^{hi} EGFP$^-$) were sorted. Allogeneic CD4$^+$ T cells (>95% purity) were isolated from spleens of Balb/c mice via negative selection of CD11c, B220, Ter119, CD8, DX5, and CD11b-expressing cells on MACS columns. Cells were cultured for 72 hr at 1:20 DC to T cell ratio, and [^{3}H]-thymidine incorporation for the last 18 hr of culture was determined via β-counter.

Gene Expression Analysis

For microarray analysis, *Gt(ROSA)26Sor*-CreER$^+$ *Tcf4*$^{flox/flox}$ mice and Cre-negative littermate controls were treated with Tmx, and 4 or 6 days later splenocytes were isolated, pooled, and enriched for lineage (CD3, CD19)-negative cells via MACS columns. The pDCs (CD11b$^-$ B220$^+$ CD11c^{lo} Bst2$^+$) were sorted directly into Trizol reagent (Invitrogen), and total RNA was reverse transcribed, amplified, labeled, and hybridized in duplicates to Mouse Genome 430 2.0 arrays (Affymetrix) as described (Cisse et al., 2008). Principal component analysis was done with the NIA Array software (Sharov et al., 2005). Normal gene expression profiles were derived from GEO data set GSE9810 (Robbins et al., 2008).

For qRT-PCR analysis, RNA from pDCs or cDCs (CD11c^{hi} Bst2$^-$) isolated as above on day 5 after Tmx treatment was reverse transcribed and assayed by SYBR Green-based real-time PCR with MX3000P instrument (Stratagene). The expression of all genes was normalized to that of β-actin and expressed relative to the indicated reference sample via the ΔΔCT method. All primers were validated for linear amplification (sequences available upon request).

Chromatin Immunoprecipitation

Cells of the human pDC lymphoma line CAL-1 (Maeda et al., 2005) were cross-linked with formaldehyde, sonicated, and subjected to immunoprecipitation with anti-E2-2 mAb (Bain et al., 1993) or mouse IgG control as described (Cisse et al., 2008). After crosslink reversal, the isolated chromatin was amplified, labeled, and hybridized to Human Promoter ChIP-on-chip Microarray Set (Agilent Technologies) according to manufacturer's instructions. Hybridized microarrays were scanned and analyzed with DNA Analytics software (Agilent Technologies).

Statistical Analysis

Statistical significance was estimated via unpaired, two-tailed Student's t test.

ACCESSION NUMBERS

The microarray data for gene expression and chromatin immunoprecipitation analysis are available in the Gene Expression Omnibus (GEO) database (http://www.ncbi.nlm.nih.gov/gds) under the accession number GSE24785.

SUPPLEMENTAL INFORMATION

Supplemental Information includes three figures and three tables and can be found with this article online at doi:10.1016/j.immuni.2010.11.023.

ACKNOWLEDGMENTS

We thank D. Holmberg, Y. Zhuang, T. Ludwig, and F. Costantini for animal strains, T. Maeda for CAL-1 cells, C. Murre for E2-2 antibody, P. Tucker and S. Jung for communicating unpublished data, and all members of the B.R. lab for help and discussions. Supported by the SPAR-American Asthma Foundation Award (B.R.), NIH awards AI072571, AI072571-S1, and AI085439 (B.R.), and NIH training awards AI007161 (K.L.L.) and GM007367 and AI080184 (B.C.).

Received: May 19, 2010
Revised: August 28, 2010
Accepted: October 14, 2010
Published online: December 9, 2010

REFERENCES

Al-Alwan, M.M., Rowden, G., Lee, T.D., and West, K.A. (2001). Fascin is involved in the antigen presentation activity of mature dendritic cells. J. Immunol. *166*, 338–345.

Bain, G., Gruenwald, S., and Murre, C. (1993). E2A and E2-2 are subunits of B-cell-specific E2-box DNA-binding proteins. Mol. Cell. Biol. *13*, 3522–3529.

Bar-On, L., Birnberg, T., Lewis, K.L., Edelson, B.T., Bruder, D., Hildner, K., Buer, J., Murphy, K.M., Reizis, B., and Jung, S. (2010). CX3CR1+ CD8alpha+ dendritic cells are a steady-state population related to plasmacytoid dendritic cells. Proc. Natl. Acad. Sci. USA *107*, 14745–14750.

Bergqvist, I., Eriksson, M., Saarikettu, J., Eriksson, B., Corneliussen, B., Grundström, T., and Holmberg, D. (2000). The basic helix-loop-helix transcription factor E2-2 is involved in T lymphocyte development. Eur. J. Immunol. *30*, 2857–2863.

Blasius, A.L., Giurisato, E., Cella, M., Schreiber, R.D., Shaw, A.S., and Colonna, M. (2006). Bone marrow stromal cell antigen 2 is a specific marker of type I IFN-producing cells in the naive mouse, but a promiscuous cell surface antigen following IFN stimulation. J. Immunol. *177*, 3260–3265.

Boursalian, T.E., Golob, J., Soper, D.M., Cooper, C.J., and Fink, P.J. (2004). Continued maturation of thymic emigrants in the periphery. Nat. Immunol. *5*, 418–425.

Cao, W., Rosen, D.B., Ito, T., Bover, L., Bao, M., Watanabe, G., Yao, Z., Zhang, L., Lanier, L.L., and Liu, Y.J. (2006). Plasmacytoid dendritic cell-specific receptor ILT7-Fc epsilonRI gamma inhibits Toll-like receptor-induced interferon production. J. Exp. Med. *203*, 1399–1405.

Cao, W., Bover, L., Cho, M., Wen, X., Hanabuchi, S., Bao, M., Rosen, D.B., Wang, Y.H., Shaw, J.L., Du, Q., et al. (2009). Regulation of TLR7/9 responses

in plasmacytoid dendritic cells by BST2 and ILT7 receptor interaction. J. Exp. Med. *206*, 1603–1614.

Caton, M.L., Smith-Raska, M.R., and Reizis, B. (2007). Notch-RBP-J signaling controls the homeostasis of CD8- dendritic cells in the spleen. J. Exp. Med. *204*, 1653–1664.

Cisse, B., Caton, M.L., Lehner, M., Maeda, T., Scheu, S., Locksley, R., Holmberg, D., Zweier, C., den Hollander, N.S., Kant, S.G., et al. (2008). Transcription factor E2-2 is an essential and specific regulator of plasmacytoid dendritic cell development. Cell *135*, 37–48.

Cobaleda, C., Jochum, W., and Busslinger, M. (2007). Conversion of mature B cells into T cells by dedifferentiation to uncommitted progenitors. Nature *449*, 473–477.

Corcoran, L., Ferrero, I., Vremec, D., Lucas, K., Waithman, J., O'Keeffe, M., Wu, L., Wilson, A., and Shortman, K. (2003). The lymphoid past of mouse plasmacytoid cells and thymic dendritic cells. J. Immunol. *170*, 4926–4932.

Crozat, K., Guiton, R., Guilliams, M., Henri, S., Baranek, T., Schwartz-Cornil, I., Malissen, B., and Dalod, M. (2010). Comparative genomics as a tool to reveal functional equivalences between human and mouse dendritic cell subsets. Immunol. Rev. *234*, 177–198.

D'Cruz, L.M., Knell, J., Fujimoto, J.K., and Goldrath, A.W. (2010). An essential role for the transcription factor HEB in thymocyte survival, Tcra rearrangement and the development of natural killer T cells. Nat. Immunol. *11*, 240–249.

Gilliet, M., Cao, W., and Liu, Y.J. (2008). Plasmacytoid dendritic cells: Sensing nucleic acids in viral infection and autoimmune diseases. Nat. Rev. Immunol. *8*, 594–606.

Grouard, G., Rissoan, M.C., Filgueira, L., Durand, I., Banchereau, J., and Liu, Y.J. (1997). The enigmatic plasmacytoid T cells develop into dendritic cells with interleukin (IL)-3 and CD40-ligand. J. Exp. Med. *185*, 1101–1111.

Hacker, C., Kirsch, R.D., Ju, X.S., Hieronymus, T., Gust, T.C., Kuhl, C., Jorgas, T., Kurz, S.M., Rose-John, S., Yokota, Y., and Zenke, M. (2003). Transcriptional profiling identifies Id2 function in dendritic cell development. Nat. Immunol. *4*, 380–386.

Iparraguirre, A., Tobias, J.W., Hensley, S.E., Masek, K.S., Cavanagh, L.L., Rendl, M., Hunter, C.A., Ertl, H.C., von Andrian, U.H., and Weninger, W. (2008). Two distinct activation states of plasmacytoid dendritic cells induced by influenza virus and CpG 1826 oligonucleotide. J. Leukoc. Biol. *83*, 610–620.

Kee, B.L. (2009). E and ID proteins branch out. Nat. Rev. Immunol. *9*, 175–184.

LeibundGut-Landmann, S., Waldburger, J.M., Reis e Sousa, C., Acha-Orbea, H., and Reith, W. (2004). MHC class II expression is differentially regulated in plasmacytoid and conventional dendritic cells. Nat. Immunol. *5*, 899–908.

Lin, Y.C., Jhunjhunwala, S., Benner, C., Heinz, S., Welinder, E., Mansson, R., Sigvardsson, M., Hagman, J., Espinoza, C.A., Dutkowski, J., et al. (2010). A global network of transcription factors, involving E2A, EBF1 and Foxo1, that orchestrates B cell fate. Nat. Immunol. *11*, 635–643.

Liu, Y.J. (2005). IPC: professional type 1 interferon-producing cells and plasmacytoid dendritic cell precursors. Annu. Rev. Immunol. *23*, 275–306.

Liu, K., and Nussenzweig, M.C. (2010). Origin and development of dendritic cells. Immunol. Rev. *234*, 45–54.

Liu, P., Keller, J.R., Ortiz, M., Tessarollo, L., Rachel, R.A., Nakamura, T., Jenkins, N.A., and Copeland, N.G. (2003). Bcl11a is essential for normal lymphoid development. Nat. Immunol. *4*, 525–532.

Liu, K., Waskow, C., Liu, X., Yao, K., Hoh, J., and Nussenzweig, M. (2007). Origin of dendritic cells in peripheral lymphoid organs of mice. Nat. Immunol. *8*, 578–583.

Maeda, T., Murata, K., Fukushima, T., Sugahara, K., Tsuruda, K., Anami, M., Onimaru, Y., Tsukasaki, K., Tomonaga, M., Moriuchi, R., et al. (2005). A novel plasmacytoid dendritic cell line, CAL-1, established from a patient with blastic natural killer cell lymphoma. Int. J. Hematol. *81*, 148–154.

Marafioti, T., Paterson, J.C., Ballabio, E., Reichard, K.K., Tedoldi, S., Hollowood, K., Dictor, M., Hansmann, M.L., Pileri, S.A., Dyer, M.J., et al. (2008). Novel markers of normal and neoplastic human plasmacytoid dendritic cells. Blood *111*, 3778–3792.

Merad, M., and Manz, M.G. (2009). Dendritic cell homeostasis. Blood *113*, 3418–3427.

Nagasawa, M., Schmidlin, H., Hazekamp, M.G., Schotte, R., and Blom, B. (2008). Development of human plasmacytoid dendritic cells depends on the combined action of the basic helix-loop-helix factor E2-2 and the Ets factor Spi-B. Eur. J. Immunol. *38*, 2389–2400.

Naik, S.H., Sathe, P., Park, H.Y., Metcalf, D., Proietto, A.I., Dakic, A., Carotta, S., O'Keeffe, M., Bahlo, M., Papenfuss, A., et al. (2007). Development of plasmacytoid and conventional dendritic cell subtypes from single precursor cells derived in vitro and in vivo. Nat. Immunol. *8*, 1217–1226.

O'Keeffe, M., Hochrein, H., Vremec, D., Caminschi, I., Miller, J.L., Anders, E.M., Wu, L., Lahoud, M.H., Henri, S., Scott, B., et al. (2002). Mouse plasmacytoid cells: Long-lived cells, heterogeneous in surface phenotype and function, that differentiate into CD8(+) dendritic cells only after microbial stimulus. J. Exp. Med. *196*, 1307–1319.

Onai, N., Obata-Onai, A., Schmid, M.A., Ohteki, T., Jarrossay, D., and Manz, M.G. (2007). Identification of clonogenic common Flt3+M-CSFR+ plasmacytoid and conventional dendritic cell progenitors in mouse bone marrow. Nat. Immunol. *8*, 1207–1216.

Pelayo, R., Hirose, J., Huang, J., Garrett, K.P., Delogu, A., Busslinger, M., and Kincade, P.W. (2005). Derivation of 2 categories of plasmacytoid dendritic cells in murine bone marrow. Blood *105*, 4407–4415.

Reizis, B. (2010). Regulation of plasmacytoid dendritic cell development. Curr. Opin. Immunol. *22*, 206–211.

Robbins, S.H., Walzer, T., Dembélé, D., Thibault, C., Defays, A., Bessou, G., Xu, H., Vivier, E., Sellars, M., Pierre, P., et al. (2008). Novel insights into the relationships between dendritic cell subsets in human and mouse revealed by genome-wide expression profiling. Genome Biol. *9*, R17.

Schmid, M.A., Kingston, D., Boddupalli, S., and Manz, M.G. (2010). Instructive cytokine signals in dendritic cell lineage commitment. Immunol. Rev. *234*, 32–44.

Sharov, A.A., Dudekula, D.B., and Ko, M.S. (2005). A web-based tool for principal component and significance analysis of microarray data. Bioinformatics *21*, 2548–2549.

Shigematsu, H., Reizis, B., Iwasaki, H., Mizuno, S., Hu, D., Traver, D., Leder, P., Sakaguchi, N., and Akashi, K. (2004). Plasmacytoid dendritic cells activate lymphoid-specific genetic programs irrespective of their cellular origin. Immunity *21*, 43–53.

Shortman, K., and Heath, W.R. (2010). The CD8+ dendritic cell subset. Immunol. Rev. *234*, 18–31.

Soumelis, V., and Liu, Y.J. (2006). From plasmacytoid to dendritic cell: Morphological and functional switches during plasmacytoid pre-dendritic cell differentiation. Eur. J. Immunol. *36*, 2286–2292.

Spits, H., Couwenberg, F., Bakker, A.Q., Weijer, K., and Uittenbogaart, C.H. (2000). Id2 and Id3 inhibit development of CD34(+) stem cells into predendritic cell (pre-DC)2 but not into pre-DC1. Evidence for a lymphoid origin of pre-DC2. J. Exp. Med. *192*, 1775–1784.

Srinivas, S., Watanabe, T., Lin, C.S., William, C.M., Tanabe, Y., Jessell, T.M., and Costantini, F. (2001). Cre reporter strains produced by targeted insertion of EYFP and ECFP into the ROSA26 locus. BMC Dev. Biol. *1*, 4.

Steinman, R.M., and Idoyaga, J. (2010). Features of the dendritic cell lineage. Immunol. Rev. *234*, 5–17.

Swiecki, M., and Colonna, M. (2010). Unraveling the functions of plasmacytoid dendritic cells during viral infections, autoimmunity, and tolerance. Immunol. Rev. *234*, 142–162.

Villadangos, J.A., and Young, L. (2008). Antigen-presentation properties of plasmacytoid dendritic cells. Immunity *29*, 352–361.

Welner, R.S., Esplin, B.L., Garrett, K.P., Pelayo, R., Luche, H., Fehling, H.J., and Kincade, P.W. (2009). Asynchronous RAG-1 expression during B lymphopoiesis. J. Immunol. *183*, 7768–7777.

Williams, L.M., and Rudensky, A.Y. (2007). Maintenance of the Foxp3-dependent developmental program in mature regulatory T cells requires continued expression of Foxp3. Nat. Immunol. *8*, 277–284.

Xie, H., Ye, M., Feng, R., and Graf, T. (2004). Stepwise reprogramming of B cells into macrophages. Cell *117*, 663–676.

Young, L.J., Wilson, N.S., Schnorrer, P., Proietto, A., ten Broeke, T., Matsuki, Y., Mount, A.M., Belz, G.T., O'Keeffe, M., Ohmura-Hoshino, M., et al. (2008). Differential MHC class II synthesis and ubiquitination confers distinct antigen-presenting properties on conventional and plasmacytoid dendritic cells. Nat. Immunol. *9*, 1244–1252.

Zhuang, Y., Cheng, P., and Weintraub, H. (1996). B-lymphocyte development is regulated by the combined dosage of three basic helix-loop-helix genes, E2A, E2-2, and HEB. Mol. Cell. Biol. *16*, 2898–2905.

Zuniga, E.I., McGavern, D.B., Pruneda-Paz, J.L., Teng, C., and Oldstone, M.B. (2004). Bone marrow plasmacytoid dendritic cells can differentiate into myeloid dendritic cells upon virus infection. Nat. Immunol. *5*, 1227–1234.